



Wideband polarization-insensitive metamaterial perfect absorber based on bilayer graphene metasurface

Bahareh Khodadadi¹ · Pejman Rezaei² · Vahid Ghods¹ · Majid Babaeinik¹

Received: 31 October 2021 / Accepted: 22 August 2022 / Published online: 16 September 2022
© The Author(s), under exclusive licence to Springer Science+Business Media, LLC, part of Springer Nature 2022, corrected publication 2022

Abstract

In this article a polarization-insensitive broadband adjustable THz metamaterial absorber is proposed and examined. The absorber is constructed of a periodic array of patterned graphene elements that is like the star as unit cell, placed on a SiO₂ dielectric layer and it is terminated by a gold reflector. The simulation results display that the proposed absorber with single graphene layer has bandwidth of 1.96 THz for absorption above 90% with the peak absorption of 98.45% in 4.18 THz. This absorber with two graphene layers covers the frequency range of 2.99–6.16 THz for absorption > 90% with the highest absorption of 99.99% at 5.30 THz. The bandwidth for absorption above 99% is 0.72 THz. The absorption curves for TE and TM modes similar together. The electric fields and current surface of proposed absorber have been investigated on low and peak absorption frequency in TE and TM modes. This structure has features such as polarization independent for normal incident waves owing to its symmetric structure, good bearing angle of incident wave and adjustable by altering the Fermi level of graphene. Due to these properties, the broadband metamaterial perfect absorber is suitable for applications such as camouflage systems, imaging, detector, energy harvesting, and modulators.

Keywords Terahertz · Metamaterial perfect absorber · Broadband · Polarization insensitive

1 Introduction

Currently, there is a superb attention in creating metamaterials that have extraordinary electromagnetic properties that are not found in nature and are different from normal materials. Fundamentally, the theory of metamaterial is achieved from the substitution of normal materials with synthetic materials more smaller than the wavelength of the incoming electromagnetic waves (Sabah et al. 2018). Interesting properties of metamaterials are achieved from the skill in its structure design such as geometry, pattern and orientation of metamaterial while its chemical structure acts a much smaller role (Lapine et al. 2009; Sabah et al.

✉ Pejman Rezaei
prezaei@semnan.ac.ir

¹ Department of Electrical Engineering, Semnan Branch, Islamic Azad University, Semnan, Iran

² Semnan University, Semnan, Iran

2018). For the first time, in 1986 Vesalago offered the material with negative refractive index that concurrently permittivity coefficient and permeability coefficient are negative in it (Vesalago 1967). Then in 1999 Smith et al. display existence of the first metamaterial with both negative electric permittivity and magnetic permeability (Smith et al. 2000). Following these works, many researchers have been turning their attention to this field for various applications, and so far many articles have been published on the use of metamaterials in the microwave (Jokanović et al. 2010; Ghods and Rezaei 2018), infrared (Lee et al. 2019; Barzegar-Parizi 2018), terahertz frequencies (Razani and Rezaei 2022; Aghaee and Orouji 2021; Jianjun Liu et al. 2016) and the range of light spectrum (Xu et al. 2011). Metamaterials play an important role in terahertz perfect absorber designing. A terahertz absorber is an essential device for detecting a terahertz-wave as many of the device, expanded for microwave sensing (Tonouchi 2007; Mishra and Panwar 2020). First nearly perfect absorber was represented by Landy et al. in 2008 (Landy et al. 2008). Then many researchers have tried to make the metamaterial absorber with a high absorption rate that is insensitive to the polarization and angle of the wave and also have the least complexity in the design and structure. Among these researches, broadband absorbers have fascinated much attention due to their wide and special applications in detection (Jun Wang et al. 2014a, b; Ebrahimi 2020), sensors (Yahiaoui et al. 2015; Soheilifar 2018), modulators (Savo et al. 2014), thermal emitters (Diem et al. 2009), and camouflage apparatuses (Haofei Shi et al. 2011).

Graphene is the name of a material formed using a two-dimensional honeycomb structure. It has emerged as one of the most important and practical metamaterials due to its exceptional electrical, thermal and optical features which makes it a good choice for next generation technology (Baringhaus et al. 2014; Mishra and Panwar 2020). Graphene is not only one of the thinnest materials but also one of the strongest materials. It transfers heat well and it is a very good conductor. It can be adjusted according to the intended application because the chemical potential of graphene can be changed by external bias voltage or chemical doping. This feature is used to design the antennas and terahertz absorbers because polarization can be controlled by altering the Fermi level of the graphene (Jafari Chashmi et al. 2020; Kiani et al. 2021; Zamzam et al. 2021). Different sorts of metamaterial absorbers have been designing based on alternating structure of graphene disks (Fengling Wang et al. 2018; Arik et al. 2017), graphene ribbons (Barzegar-Parizi 2019; Xiao et al. 2018; Alaei et al. 2012) and graphene fishnets (Andryeuskii and Lavrinenko 2013) that act as an narrowband absorber. The bandwidth of absorber significantly affects its applications. The narrowband absorbers restrict area of usage. Actually, metamaterial perfect absorber over a wide spectral range is more practical (Jindal and Kumar 2015). Generally, two methods or strategies are proposed to obtain broadband metamaterial absorber: (1) forming coplanar structure (Lu et al. 2018; Huang et al. 2016, 2015; Viet et al. 2014), and (2) stacking multiple metamaterial or metal, and dielectric layers alternately in the direction of propagation of the electromagnetic waves (Ding et al. 2011; Cui et al. 2012; Wang et al. 2014a, b; Liu et al. 2015). However, in the coplanar structures, there are multiple interactions between subunits in them. Thus, the major challenge to design a broadband perfect absorber is excellent adsorption conditions that are easily broken by their interactions. Also, several stacked structures suffer from production problems. Consequently, perfect broadband absorbers, which have a variety of applications, still are an important subject in the field of metamaterials (Xiao et al. 2017).

In this paper, two version of broadband terahertz perfect absorbers are proposed. Initially, first absorber consists of three layers, the gold as the ground layer and a patterned graphene in the top layer. The layer of SiO₂ separates the two layers. The structure of this absorber is not complex and due to its symmetrical design, it's not sensitive to polarization. The bandwidth of

this structure for absorption above 90% is equal to 1.96THz. Then by putting on second layer of graphene, a wider absorber is obtained. Subsequently, the absorber feature is investigated and the effect of different parameters such as Fermi levels, permittivity of dielectric, relaxation time, incident angle and polarization on the proposed structure is examined. Finally, the electric fields and current surface of absorbers are evaluated. Then, by adding the test medium in the top of the absorber, we have examined it for application in the refractive index sensor.

2 Structure design and simulation

The proposed metamaterial absorber contains three layers as display in Fig. 1a, b. The bottom layer is made of gold with conductivity of $\sigma_{gold} = 4.56 \times 10^7$ and a thickness is $h_g = 0.1\mu\text{m}$ which is larger than its typical skin depth (Zamzam and Rezaei 2021). Gold is chosen as a perfect reflective metal plane. The middle layer is SiO_2 with the relative electric permittivity of $\epsilon_r = 2.25$ (Deng et al. 2014) and the height of substrate layer is $h_d = 10\mu\text{m}$. The top layer of the unit cell of the graphene pattern has displayed in Fig. 1c. The dimension of the graphene used in top layer are given as follows: $p_x = p_y = 3\mu\text{m}$, the width of the arms of the cross $a = 0.4\mu\text{m}$ and its length is $b = 2.6\mu\text{m}$. The thickness of graphene is equal to 1 nm. Also, to upgrade the system, according to Fig. 1d, e, another layer of graphene with the same pattern and a dielectric separator SiO_2 with $h_s = 2\mu\text{m}$ have been added to the desired structure.

In the current research, effective surface conductivity is generally used to describe the properties of graphene. The graphene surface conductivity including intraband and interband electron transitions that can be expressed by using the Hanson formula (Xiao-Peng et al. 2012):

$$\sigma_g(\omega \cdot \mu_c \cdot \Gamma \cdot T) = N_g(\sigma_{intra} + \sigma_{inter}) \tag{1}$$

$$\sigma_{intra} = \frac{ie^2k_B T}{\pi\hbar^2(\omega + 2i\Gamma)} \left[\frac{\mu_c}{k_B T} + 2 \ln \left(1 + e^{\frac{\mu_c}{k_B T}} \right) \right]$$

$$\sigma_{inter} = \frac{ie^2}{4\pi\hbar^2} \ln \left[\frac{2|\mu_c| - (\omega + 2i\Gamma)\hbar}{2|\mu_c| + (\omega + 2i\Gamma)\hbar} \right]$$

The relative dielectric constant is expressed as (SHI and CUI 2020):

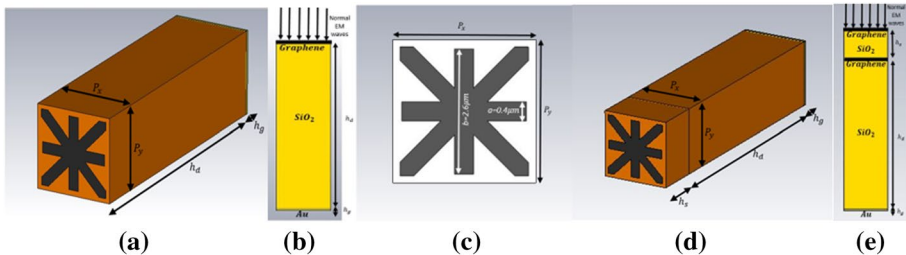


Fig. 1 **a** Schematic diagram of the metamaterial perfect absorber, $p_x = p_y = 3 \mu\text{m}$, $h_d = 10 \mu\text{m}$, $h_g = 0.1 \mu\text{m}$, **b** Side view and **c** Top view of the absorber with single graphene layer, **d** Structure of the metamaterial perfect absorber with two graphene layers, $h_s = 2 \mu\text{m}$ **e** Side view of absorber with two graphene layer

$$\varepsilon_g = 1 + \frac{i\sigma_g}{\omega\varepsilon_0 N_g t_g} \quad (2)$$

graphene surface conductivity relies on $\omega = 2\pi f$, μ_c , $\Gamma = 1/2\tau$ and T where ω , μ_c , Γ and $T=300$ are radian angular frequency, relaxation time, chemical potential and absolute temperature respectively.

Also N_g is number of graphene layers, k_B is the Boltzmann constant, \hbar is the reduced Planck constant, e is the elementary charge and ε_0 is the vacuum dielectric constant. When graphene has a chemical potential of $|\mu_c| \ll \hbar\omega/2$, the inter-band conductivity σ_{inter} plays a dominant role, and the in-band conductivity σ_{intra} can be ignored. When the chemical potential $|\mu_c| \gg \hbar\omega/2$, the in-band conductivity σ_{intra} plays influential role, and when the band is below 30 THz and the chemical potential is above 0.1 eV, the σ_{inter} can be ignored according to the Pauli principle of incompatibility (Teperik et al. 2008). The conductivity of graphene is only expressed using the in-band conductivity. So, the graphene surface conductivity could be changed to a Drude-like model (Tongling Wang et al. 2020)

$$\sigma_g(\omega) = \frac{ie^2\mu_c}{\pi h^2(\omega + i\tau^{-1})} \quad (3)$$

In the proposed absorbers $E_f=0.9$ eV and $\tau=0.1$ ps (Zamzam et al. 2021).

To validate the absorber efficiency, the model is simulated by using the frequency domain solver in CST Microwave Studio by using a hexahedral mesh. The boundary condition of the unit cell was employed along the $x-y$ axis. To set the boundary conditions, the x/y directions of the unit cell are specified as periodic and an open boundary in the z direction is considered. The wave of the electromagnetic plane in the z direction was modeled as a Floquet port with a polarization in the y direction. The absorption could be obtained as

$$A = 1 - R - T = 1 - |S_{11}|^2 - |S_{21}|^2 \quad (4)$$

where R and T demonstrate the reflectance and transmittance, respectively. As mentioned, because the height of the bottom layer is much more than the skin depth, the absorption could be calculated by $A = 1 - R$ (Patel et al. 2020).

3 Result and discussion

We simulated the structure under normal incidence in TE and TM waves. As demonstrated in Fig. 2a, the proposed absorber has a bandwidth of 1.96 THz in absorption above 90% with the peak absorption in 4.1869 THz. Then, as mentioned before, this broadband perfect absorber is improved by adding another layer of graphene with the same pattern and parameter. This layer is separated with another layer of SiO_2 with width of $h_s = 2 \mu\text{m}$ from previous layer of graphene. These changes have increased the absorption bandwidth about 61.73% for absorption above 0.9 as depicted in Fig. 2b. The broadband perfect absorber covers frequency from 2.99 to 6.16 THz for absorption >90% and 3.25–5.84 THz for absorption >97% and 4.90–5.62 THz for absorption >99%. As demonstrated in Fig. 2, the TE polarization absorption curve are exactly similar to the TM polarization absorption curve, which outcome from the symmetric geometry of the structure.

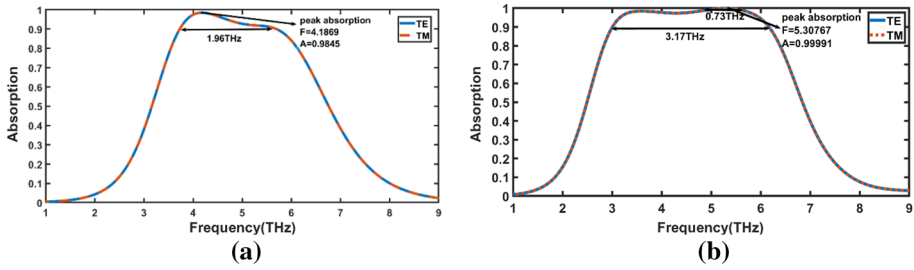


Fig. 2 Absorption spectra of structure **a** with single graphene layer in the normal incidence of TE/TM waves when Fermi level is 0.9 eV and relaxation time is 0.1 ps, **b** with two graphene layers in the normal incidence of TE/TM waves when Fermi level is 0.9 eV and relaxation time is 0.1 ps

One of the advantages of this absorber is that the absorption frequency can be adjusted for the intended application without altering the structure geometry, only by altering Fermi level (μ_c) of graphene. The surface conductivity of graphene increases with increasing μ_c , as shown by Eq. (3). As depicted in the Fig. 3, by increasing the Fermi level, the absorption frequency is blue shifted, value of absorption is increased and the absorption peak frequencies are transmitted to higher frequencies. As the μ_c increases, the concentration of the carrier increases, which leads to stronger excitation (Li et al. 2019). As a result, the absorption efficiency is improved. The Fermi level of graphene sheet can be calculated by using Eq. (5) (Nickpay et al. 2022) as shown below.

$$\mu_c = \hbar v_F \sqrt{\pi C V_{DC} / q_e} \tag{5}$$

Here V_{DC} is the gate voltage, $v_F = 9.5 \times 10^5 m/s$ is the Fermi velocity, C is the capacitance and is given by $C = \epsilon_d \epsilon_0 / h_r \epsilon_d$ is electric permittivity, ϵ_0 is permittivity of free space and h is dielectric layer thickness. So, the μ_c can be changed by applying an external DC bias voltage, which directly affects the conductivity of the graphene layer and it can be influence the designed system.

Also, the changing in the relative electric permittivity dielectric parameter (ϵ_r) was investigated in Fig. 4. We kept other parameters fixed and only change the relative

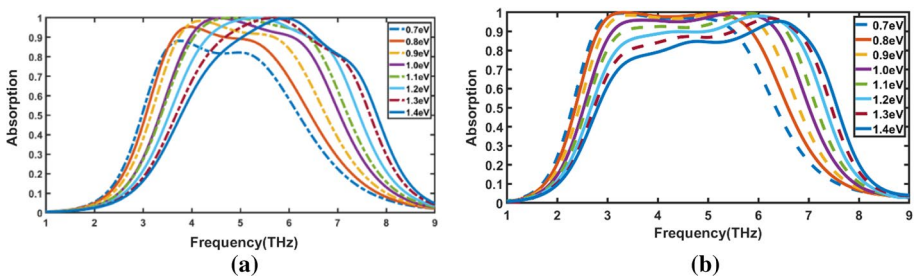


Fig. 3 Absorption spectra of structure for different Fermi level of graphene **a** single layer of graphene, **b** two graphene layers

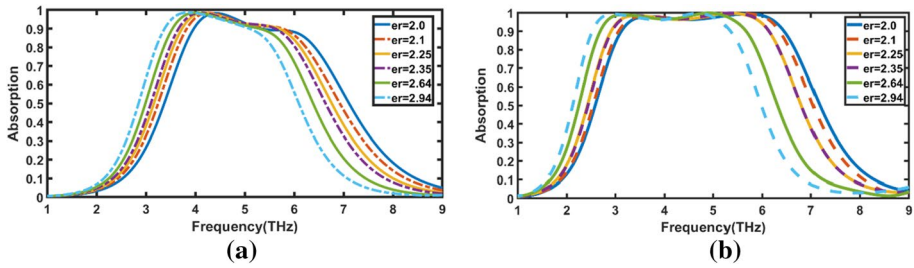


Fig. 4 Absorption spectra of structure for different relative electric permittivity of dielectric, **a** single layer of graphene, **b** two graphene layers

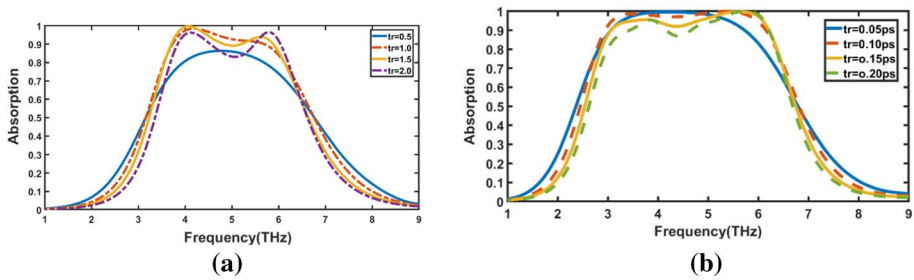


Fig. 5 Absorption spectra of structure for different relaxation time of graphene, **a** single layer of graphene, **b** two graphene layers

electric permittivity of dielectric (ϵ_r). This investigation shows that by reducing the values of ϵ_r , the absorption frequency decrease and vice versa. According to relation

$$\varphi_p = \frac{4h\sqrt{\epsilon_r - \sin^2\theta}}{\lambda} \tag{6}$$

where h is the thickness of dielectric layer and φ_p is phase path of incident wave. Plane wave is transferred on the homogeneous medium layer at normal incident, so θ and φ_p is constant. Therefore the shift of the frequency relies on ϵ_r (Zamzam et al. 2021). Another parameter of graphene that can be affected the frequency of absorption spectra is relaxation time. Factors affecting the relaxation time of graphene has been shown in Eq. (7), where ν and V_F respectively represent electron mobility and Fermi velocity (approximately $10^6 m/s$).

$$\tau = \nu\mu_c / eV_F^2 \tag{7}$$

Therefore, by altering the relaxation time, the absorption spectrum of structure can be tuned, as you can see in Fig. 5.

For an ideal absorber, the values of absorption and absorption spectra remain unchanged for any state of polarization and angle of incidence of an EM-wave (Aydin et al. 2011). However, controlling minor changes in the absorber performance is a challenging task. Fluctuations observed in absorption at a given radiation angle may be due to

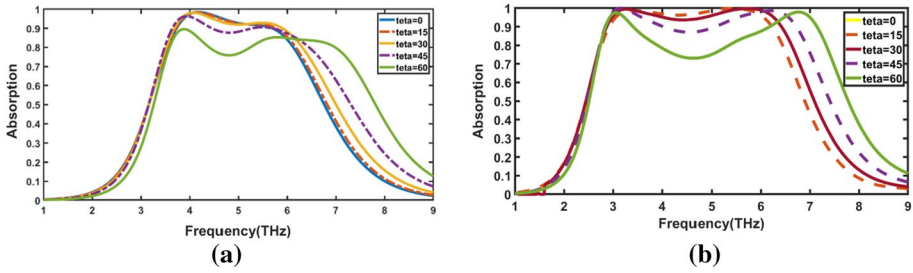


Fig. 6 Absorption spectra of structure for different incidence angles, **a** single layer of graphene, **b** two graphene layers

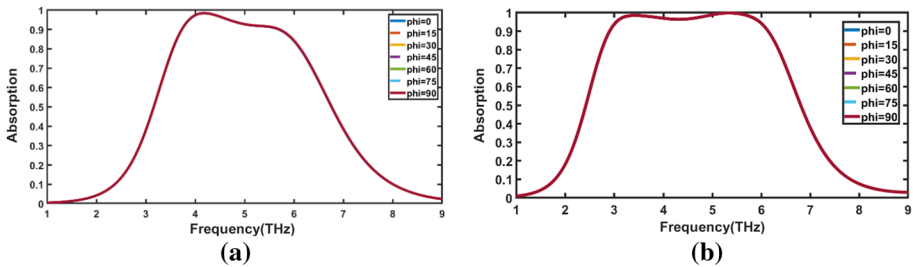


Fig. 7 Absorption spectra of structure for different polarization angles, **a** single layer of graphene, **b** two graphene layers

the occurrence of impedance mismatch, which increases the reflection of the incident wave (He et al. 2011). Figure 6 displays the absorption when the incident angle increases. The θ represents the incident angle of the TE waves and TM waves. It is interesting to notice that a slight shift in the absorption spectra appears as the incident angle varies. As you can see, with increasing incident angle, the rate of absorption is decreased because more diagonal incidence increases reflection. So up to $\theta = 60^\circ$, we have a wide-angle absorber. We characterized the polarization dependent of absorption for the proposed structure under normal incidence. In Fig. 7, φ_p represents the angle between the polarization direction of the incident THz wave and y direction. It is clear from the Fig. 7 that the proposed structure has maintained excellent absorption stability at different angles of polarization. The structure gives the same result in response to the different polarization of the waves. This is achieved by utilizing a symmetric resonator. When the incident waves strike a symmetric resonator at different angles, the resonator behaves similarly and provides the same response. This is considered as the basic mechanism of independent polarization for symmetrical structures.

Then we investigate the influence of two major parameters of structure (dielectric layers thickness) h_s and h_d on the absorption characteristic, from Fig. 8a, b, one can see that the change of the h_s and h_d slightly affects the absorptivity and the bandwidth, while the change of h_d has an evident influence on the absorption. As h_d increases, the absorption bandwidth is slowly stretched toward a lower frequency where the absorptivity is gradually decreased. Figure 8a presents the effect of the dielectric layer thickness h_s on the absorber characteristics as the dielectric thickness increases, the absorption bandwidth becomes narrower and blue-shift, while the value of absorption slightly decreases. For

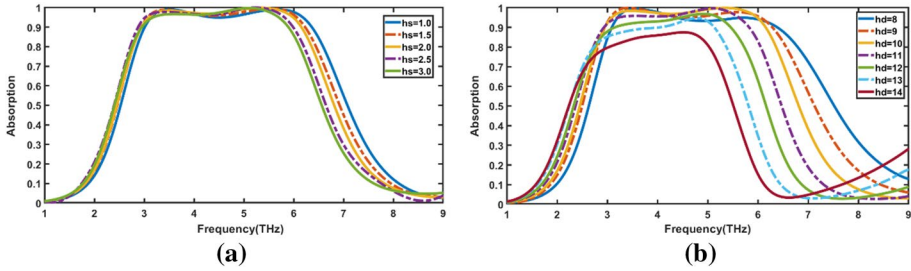


Fig. 8 Absorption spectra of structure for different values of **a** h_s and **b** h_d

a compromise consideration of the absorptivity and bandwidth, we choose the thickness of dielectric $h_d = 10 \mu\text{m}$ and $h_s = 2 \mu\text{m}$ in this work.

In the next step, to check the mechanism of the absorption for the structure with single graphene layer, we plotted the electric fields distribution under the normal incidence of TE and TM waves at the peak absorption frequency at $f = 4.93 \text{ THz}$ and at the lower absorption frequency at $f = 3 \text{ THz}$. As displayed in Fig. 9 for the single layer of graphene, at $f = 4.93 \text{ THz}$ the electric fields are mostly concentrated at the end of the star strings in the corner of unit cell, and at $f = 3 \text{ THz}$, the electric fields concentration is reduced. In Fig. 10, for structure with two layers of graphene at peak absorption frequency $f = 5.3 \text{ THz}$ the electric fields are concentrated at the end of star strings in top and bottom unit cell, and in lower absorption frequency $f = 2 \text{ THz}$ the concentration of the electric fields is decreased. In TM mode, the electric fields are similar to TE mode but in other direction. Figure 11 shows the surface current distribution which is generated due to the incident electromagnetic interaction with the absorber at the peak absorption frequency at $f = 5 \text{ THz}$ and at the lower absorption frequency at $f = 2 \text{ THz}$ in TE and TM mode. It is observed that the surface current density at 5 THz is more concentrated in the center of the star-shaped layer branches. The direction of the arrows varies according to the incident wave mode (TE, TM).

For sensor application, an unknown layer is added to the proposed metamaterial absorber and simulations are performed accordingly. In order to reveal the properties of the sensor, the refractive index (RI) of the unknown layer is varied and changes in the absorption spectrum are investigated. When the test medium or analyte is added, metamaterials can analyze and investigate the unknown material by giving response in the absorption spectra. Because of the added unknown material, interaction occurs between this analyte and the metamaterial absorber. As a result of this interaction, frequency shifts occur. By analyzing these shifts, the sensing property can be realized (Sabah and Roskos 2013). For RI sensing, the refractive index (n) of the over-layer is altered between 1 and 1.8 with the step of 0.1. The thickness of the unknown layer is assumed to be $0.8 \mu\text{m}$. The absorption results corresponding to the variation of the refractive indexes are given in Fig. 12. When RI is increased, it is observed that the absorption spectrum is shifting to the left side (redshift) of the spectrum. This is because of the change in the total capacitance of the structure. It is also known that the absorption

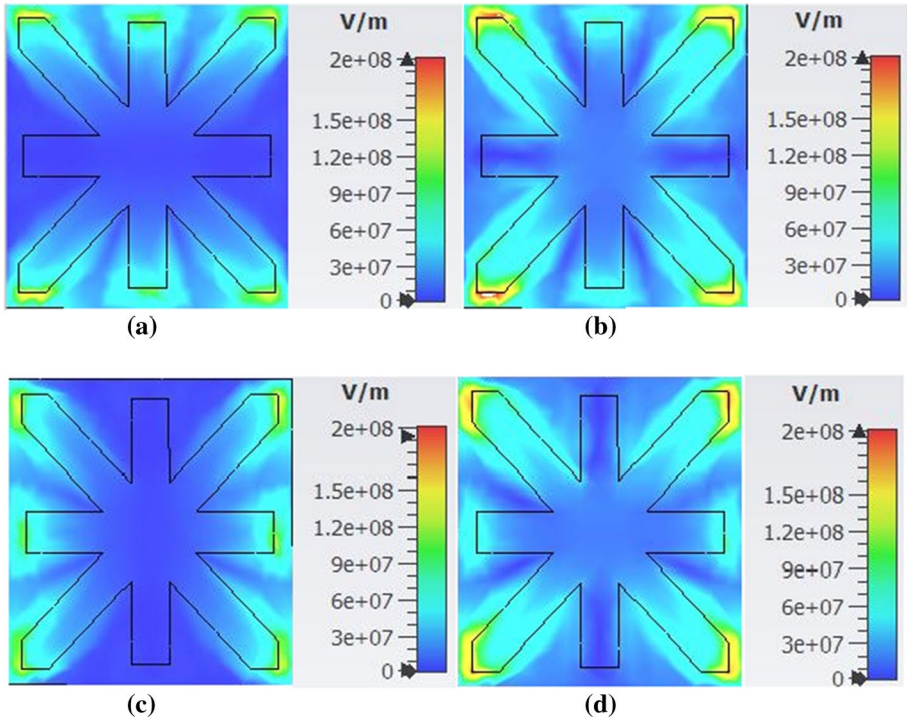


Fig. 9 Electric fields distributions in structure with single layer of graphene in the normal incidence of **a** TE waves at $f=3$ THz, **b** TE waves at $f=4.93$ THz, **c** TM waves at $f=3$ THz, **d** TM waves at $f=4.93$ THz

spectrum is strongly dependent on the total capacitance of the structure. When the test medium is added to the top of the structure, the capacitance of the design structure increases and therefore, the absorption spectrum shifts downwards (Sabah and Roskos 2013).

Finally, we have collected and compared the absorber proposed in this article with some of the absorbers presented in recent years in Table 1. As it is showed, the proposed absorber with single layer of graphene has bandwidth 1.96 for absorption above 0.9 and the absorber with two layer of graphene has bandwidth 3.17 for absorption over 90% and 0.72 for absorption over 99% that is wider than some of the absorbers presented in Table 1. Also, this absorber has the benefits of insensitivity to polarization and incident angle.

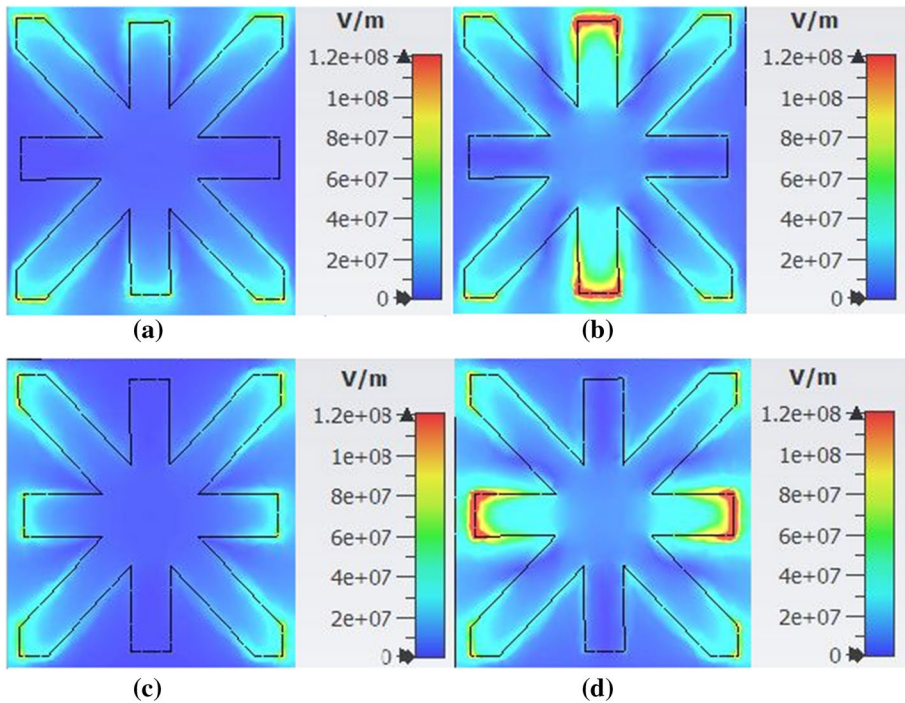


Fig. 10 Electric fields distributions in structure with two graphene layers in the normal incidence of **a** TE waves at $f=2$ THz, **b** TE waves at $f=5.3$ THz, **c** TM waves at $f=2$ THz, **d** TM waves at $f=5.3$ THz

4 Conclusion

In total, a perfect broadband THz absorber based on single graphene layer and two graphene layers have been designed and investigated. The proposed classic absorber contains three layers, the top layer is a periodic pattern of graphene and a gold plane is in the bottom layer, these layers detached by a SiO_2 dielectric layer. The simulation results have showed that under normal incidence in TE/TM waves the proposed absorber has wideband absorption from 3.73 to 5.69 THz for a single graphene layer and 2.99–6.16 THz for two graphene layers for absorption above 90% and has 3.97–4.45 THz for a single graphene layer and 3.25–5.84 THz for two graphene layer for absorption above 97% and has the bandwidth of 0.72 for two graphene layers for absorption above 0.99. These absorbers have the ability to regulate the position of the absorption bands by tuning the Fermi level of graphene without altering the dimension of the absorber structure. Also, this structure design is insensitive to polarization and incident angle up to 60° . This broadband perfect absorber proffers a new path for camouflage systems, detector, imaging, energy harvesting, and modulators.

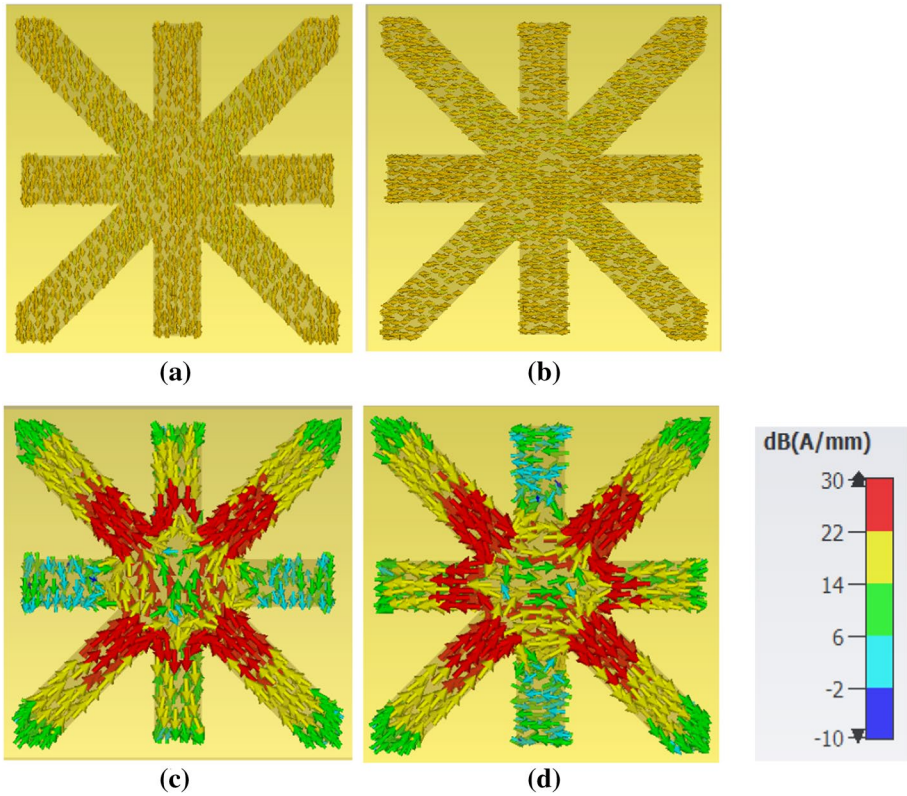


Fig. 11 Surface current distributions in structure with two graphene layers in the normal incidence **a** at $f = 2$ THz in TE mode, **b** at $f = 2$ THz in TM mode, **c** at $f = 5$ THz in TE mode, **d** at $f = 5$ THz in TE mode

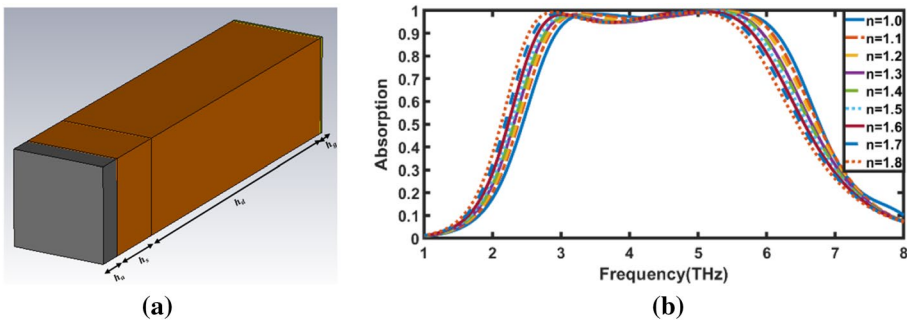


Fig. 12 **a** Schematic diagram of the metamaterial perfect absorber with test medium (analyte), $h_a = 0.8 \mu m$, **b** Variation of absorption spectra when using different RI of analyte

Table 1 Comparison between the features of the absorber of different articles with the proposed absorber in this paper

Ref. year	Bandwidth (> 90%)		Bandwidth (> 99%)		Structure layers No.	Sensitivity to polarization	Sensitivity to incident angle
	(THz)	%	(THz)	%			
Fu et al. (2018)	5.50–9.10	49.31	8.04–8.50	5.56	7	No	Wide angle
Dong et al. (2021)	1.24–2.08	50.60	0	0	5	Up to 50	NR
Feng et al. (2021)	1.10–1.86	51.35	1.23–1.68	30.92	3	No	Up to 60
Bai et al. 2019	4.3–5.5	24.48	0	0	4	No	No
Huang et al. (2018)	0.95–2.52	90.49	0	0	3	No	No
Mou et al. (2018)	0.91–1.51	49.58	1.26–1.28	1.57	5	Up to 50	No
Wang et al. (2020)	0.7–1.7	83.33	1.05–1.07	1.88	3	No	No
			1.24–1.27	2.39			
Gao et al. (2017)	1.27–2.08	48.35	1.32–1.37	3.17	4	NR	NR
Huang et al. (2018)	2.0–3.75	60.86	3.25–3.45	5.97	3	Up to 60(TE) Up to 80(TM)	No
One graphene layer	3.73–5.69	41.61	0	0	3	No	Up to 60
Two graphene layers	2.99–6.16	41.54	4.90–5.62	13.68	5	No	Up to 60

⁺NR: Not reported

References

- Aghaee, T., Orouji, A.A.: Dual-band terahertz absorber based on graphene periodic arrays of disks and ribbons: circuit model approach. *J. Comput. Electron.* **20**, 611–625 (2021)
- Alaee, R., Farhat, M., Rockstuhl, C., Lederer, F.: A perfect absorber made of a graphene micro-ribbon metamaterial. *Opt. Express* **20**, 28017–28024 (2012)
- Andryieuski, A., Lavrinenko, A.: Graphene metamaterials based tunable terahertz absorber: effective surface conductivity approach. *Opt. Express* **21**, 9144–9155 (2013)
- Arik, K., AbdollahRamezani, S., Khavasi, A.: Polarization insensitive and broadband terahertz absorber using graphene disks. *Plasmonics* **12**, 393–398 (2017)
- Aydin, K., Ferry, V.E., Briggs, R.M., Atwater, H.A.: Broadband polarization-independent resonant light absorption using ultrathin plasmonic super absorbers. *Nat. Commun.* **2**, 517 (2011)
- Bai, J., Zhang, S., Fan, F., Wang, S., Sun, X., Miao, Y., Chang, S.: Tunable broadband THz absorber using vanadium dioxide metamaterials. *Optics Commun.* **452**, 292–295 (2019)
- Baringhaus, J., Ruan, M., Edler, F., Tejeda, A., Sicot, M., Taleb-Ibrahimi, A., Li, A.-P., Jiang, Z., Conrad, E.H., Berger, C., Tegenkamp, C., De Heer, W.A.: Exceptional ballistic transport in epitaxial graphene nanoribbons. *Nature* **506**, 349–354 (2014)
- Barzegar-Parizi, S.: Realization of wide-angle and wideband absorber using metallic and graphene-based metasurface for mid-infrared and low THz frequency. *Opt. Quant. Electron.* **50**, 1–12 (2018)
- Barzegar-Parizi, S.: Graphene-based tunable dual-band absorbers by ribbon/disk array. *Opt. Quant. Electron.* **51**, 1–11 (2019)
- Cui, Y., Fung, K.H., Xu, J., Ma, H., Jin, Y., He, S., Fang, N.X.: Ultrabroadband light absorption by a sawtooth anisotropic metamaterial slab. *Nano Lett.* **12**, 1443–1447 (2012)
- Deng, X.-H., Liu, J.-T., Yuan, J., Wang, T.-B., Liu, N.-H.: Tunable THz absorption in graphene-based heterostructures. *Opt. Express* **22**, 30177–30183 (2014)
- Diem, M., Koschny, T., Soukoulis, C.M.: Wide-angle perfect absorber/thermal emitter in the terahertz regime. *Phys. Rev. B* **79**, 033101 (2009)
- Ding, F., Cui, Y., Ge, X., Jin, Y., He, S.: Ultra-broadband microwave metamaterial absorber. *Appl. Phys. Lett.* **100**, 103506 (2011)

- Dong, Y., Yu, D., Li, G., Li, G., Ma, H.: Tunable ultrathin ultrabroadband metamaterial absorber with graphene-stack-based structure at lower terahertz frequency. *Phys. E* **128**, 114608 (2021)
- Ebrahimi, S.: Optical absorber based on self-similar cylindrical element for detecting optical material. *Opt. Quant. Electron.* **52**, 1–11 (2020)
- Feng, H., Xu, Z., Li, K., Wang, M., Xie, W., Luo, Q., Chen, B., Kong, W., Yun, M.: Tunable polarization-independent and angle-insensitive broadband terahertz absorber with graphene metamaterials. *Opt. Express* **29**, 7158–7167 (2021)
- Fu, P., Liu, F., Ren, G.J., Su, F., Li, D., Yao, J.Q.: A broadband metamaterial absorber based on multi-layer graphene in the terahertz region. *Opt. Commun.* **417**, 62–66 (2018)
- Gao, F., Zhu, Z., Xu, W., Zhang, J., Guo, C., Liu, K., Yuan, X., Qin, S.: Broadband wave absorption in single-layered and nonstructured graphene based on far-field interaction effect. *Opt. Express* **25**, 9579–9586 (2017)
- Ghods, M.M., Rezaei, P.: Ultra-wideband microwave absorber based on uncharged graphene layers. *J. Electromagn. Waves Appl.* **32**, 1950–1960 (2018)
- He, X.-J., Wang, Y., Wang, J., Gui, T., Wu, Q.: Dual-band terahertz metamaterial absorber with polarization insensitivity and wide incident angle. *Prog. Electromagn. Res.* **115**, 381–397 (2011)
- Huang, X., He, X., Guo, L., Yi, Y., Xiao, B., Yang, H.: Analysis of ultra-broadband metamaterial absorber based on simplified multi-reflection interference theory. *J. Opt.* **17**, 055101 (2015)
- Huang, X., Yang, H., Wang, D., Yu, S., Lou, Y., Guo, L.: Calculations of a wideband metamaterial absorber using equivalent medium theory. *J. Phys. D Appl. Phys.* **49**, 325101 (2016)
- Huang, X., He, W., Yang, F., Ran, J., Gao, B., Zhang, W.-L.: Polarization-independent and angle-insensitive broadband absorber with a target-patterned graphene layer in the terahertz regime. *Opt. Express* **26**, 25558–25566 (2018)
- Jafari Chashmi, M., Rezaei, P., Kiani, N.: Y-shaped graphene-based antenna with switchable circular polarization. *Optik* **200**, 163321 (2020)
- Jindal, S., Kumar, M.: Broadband and polarization insensitive design of terahertz absorber with high-index contrast grating on SOI chip. *Opt. Quant. Electron.* **47**, 1693–1702 (2015)
- Jokanović, B., Geschke, R.H., Beukman, T.S., Milošević, V.: Metamaterials: characteristics, design and microwave applications. *SAIEE Afr. Res. J.* **101**, 82–92 (2010)
- Kiani, N., Hamedani, F.T., Rezaei, P.: Polarization controlling idea in graphene-based patch antenna. *Optik* **239**, 166795 (2021)
- Landy, N.I., Sajuyigbe, S., Mock, J.J., Smith, D.R., Padilla, W.J.: Perfect metamaterial absorber. *Phys. Rev. Lett.* **100**, 207402 (2008)
- Lapine, M., Powell, D., Gorkunov, M., Shadrivov, I., Marqués, R., Kivshar, Y.: Structural tunability in metamaterials. *Appl. Phys. Lett.* **95**, 084105 (2009)
- Lee, N., Kim, T., Lim, J.-S., Chang, I., Cho, H.H.: Metamaterial-selective emitter for maximizing infrared camouflage performance with energy dissipation. *ACS Appl. Mater. Interfaces.* **11**, 21250–21257 (2019)
- Li, C., Xie, B., Chen, J., He, Z., Chen, Z., Long, Y.: Emerging mineral-coupled composite phase change materials for thermal energy storage. *Energy Convers. Manag.* **183**, 633–644 (2019)
- Liu, S., Chen, H., Cui, T.: A broadband terahertz absorber using multi-layer stacked bars. *Appl. Phys. Lett.* **106**, 151601 (2015)
- Liu, J., Fan, L., Ku, J., Mao, L.: Absorber: a novel terahertz sensor in the application of substance identification. *Opt. Quantum Electron.* **48**, 80 (2016)
- Lu, Y., Li, J., Zhang, S., Sun, J., Yao, J.: Polarization-insensitive broadband terahertz metamaterial absorber based on hybrid structures. *Appl. Opt.* **57**, 6269 (2018)
- Mishra, R., Panwar, R.: Investigation of graphene fractal frequency selective surface loaded terahertz absorber. *Opt. Quantum Electron.* **52**, 1–13 (2020)
- Mou, N., Sun, S., Dong, H., Dong, S., He, Q., Zhou, L., Zhang, L.: Hybridization-induced broadband terahertz wave absorption with graphene metasurfaces. *Opt. Express* **26**, 11728–11736 (2018)
- Nickpay, M.R., Danaie, M., Shahzadi, A.: Design of a graphene-based multi-band metamaterial perfect absorber in THz frequency region for refractive index sensing. *Phys. E* **138**, 115114 (2022)
- Norouzi Razani, A., Rezaei, P.: Multiband polarization insensitive and tunable terahertz metamaterial perfect absorber based on the heterogeneous structure of graphene. *Opt. Quantum Electron.* **52**, 407 (2022)
- Patel, S.K., Charola, S., Parmar, J., Ladumor, M., Ngo, Q.M., Dhasarathan, V.: Broadband and efficient graphene solar absorber using periodical array of C-shaped metasurface. *Opt. Quantum Electron.* **52**, 1–19 (2020)
- Sabah, C., Roskos, H.G.: Broadside-coupled triangular split-ring-resonators for terahertz sensing. *Eur. Phys. J. Appl. Phys.* **61**, 30402 (2013)

- Sabah, C., Mulla, B., Altan, H., Ozyuzer, L.: Cross-like terahertz metamaterial absorber for sensing applications. *Pramana* **91**, 1–7 (2018)
- Savo, S., Shrekenhamer, D., Padilla, W.J.: Liquid crystal metamaterial absorber spatial light modulator for THz applications. *Adv. Opt. Mater.* **2**, 275–279 (2014)
- Shi, H., Ok, J.G., Won Baac, H., Jay Guo, L.: Low density carbon nanotube forest as an index-matched and near perfect absorption coating. *Appl. Phys. Lett.* **99**, 211103 (2011)
- SHI, L., CUI, T.: Research progress in terahertz metamaterials and their applications in imaging. *J. Mater. Eng.* **48**, 12–22 (2020)
- Smith, D.R., Padilla, W.J., Vier, D., Nemat-Nasser, S.C., Schultz, S.: Composite medium with simultaneously negative permeability and permittivity. *Phys. Rev. Lett.* **84**, 4184 (2000)
- Soheilifar, M.R.: Wideband optical absorber based on plasmonic metamaterial cross structure. *Opt. Quant. Electron.* **50**, 1–12 (2018)
- Teperik, T.V., García de Abajo, F.J., Borisov, A.G., Abdelsalam, M., Bartlett, P.N., Sugawara, Y., Baumberg, J.J.: Omnidirectional absorption in nanostructured metal surfaces. *Nature Photon.* **2**(5), 299–301 (2008)
- Tonouchi, M.: Cutting-edge terahertz technology. *Nat. Photonics* **1**, 97–105 (2007)
- Veselago, V.G.: Electrodynamics of substances with simultaneously negative and. *Usp. Fiz. Nauk.* **92**, 517 (1967)
- Viet, D.T., Hien, N.T., Tuong, P.V., Minh, N.Q., Trang, P.T., Le, L.N., Lee, Y.P., Lam, V.D.: Perfect absorber metamaterials: peak, multi-peak and broadband absorption. *Opt. Commun.* **322**, 209–213 (2014)
- Wang, B., Wang, L., Wang, G., Huang, W., Li, X., Zhai, X.: Theoretical investigation of broadband and wide-angle terahertz metamaterial absorber. *IEEE Photonics Technol. Lett.* **26**, 111–114 (2014a)
- Wang, J., Gou, J., Li, W.: Preparation of room temperature terahertz detector with lithium tantalate crystal and thin film. *AIP Adv.* **4**, 027106 (2014b)
- Wang, F., Huang, S., Li, L., Chen, W., Xie, Z.: Dual-band tunable perfect metamaterial absorber based on graphene. *Appl. Opt.* **57**, 6916–6922 (2018)
- Wang, T., Zhang, Y., Zhang, H., Cao, M.: Dual-controlled switchable broadband terahertz absorber based on a graphene-vanadium dioxide metamaterial. *Opt. Mater. Express* **10**, 369–386 (2020)
- Xiao, B., Gu, M., Qin, K., Xiao, S.: Absorption enhancement in graphene with an efficient resonator. *Opt. Quant. Electron.* **49**, 177 (2017)
- Xiao, B., Lin, H., Xiao, L., Gu, M., Yang, D., Hu, L., Guo, F., Mi, H.: A tunable dual-band THz absorber based on graphene sheet and ribbons. *Opt. Quantum Electron.* **50**, 1–8 (2018)
- Xiao-Peng, S., Tie-Jun, C., Jian-Xiang, Y.: Dual band metamaterial absorber in microwave regime. *Acta Phys. Sin.* **61**, 058101 (2012)
- Xu, X., Peng, B., Li, D., Zhang, J., Wong, L.M., Zhang, Q., Wang, S., Xiong, Q.: Flexible visible–infrared metamaterials and their applications in highly sensitive chemical and biological sensing. *Nano Lett.* **11**, 3232–3238 (2011)
- Yahiaoui, R., Tan, S., Cong, L., Singh, R., Yan, F., Zhang, W.: Multispectral terahertz sensing with highly flexible ultrathin metamaterial absorber. *J. Appl. Phys.* **118**, 083103 (2015)
- Zamzam, P., Rezaei, P.: A terahertz dual-band metamaterial perfect absorber based on metal-dielectric-metal multi-layer columns. *Opt. Quantum Electron.* **53**, 1–9 (2021)
- Zamzam, P., Rezaei, P., Khatami, S.A.: Quad-band polarization-insensitive metamaterial perfect absorber based on bilayer graphene metasurface. *Phys. E* **128**, 114621 (2021)

Publisher's Note Springer Nature remains neutral with regard to jurisdictional claims in published maps and institutional affiliations.

Springer Nature or its licensor holds exclusive rights to this article under a publishing agreement with the author(s) or other rightsholder(s); author self-archiving of the accepted manuscript version of this article is solely governed by the terms of such publishing agreement and applicable law.